JOURNAL OF Materials CHEMISTRY

Palladium-containing polyaniline and polypyrrole microparticles

S. W. Huang,[a] **K. G. Neoh,**[a]*† **E. T. Kang,**[a] **H. S. Han**[b] **and K. L. Tan**[b]

[a] *Department of Chemical Engineering, National University of Singapore, Kent Ridge, Singapore 119260*

[b] *Department of Physics, National University of Singapore, Kent Ridge, Singapore 119260*

The synthesis of palladium-containing electroactive polymer microparticles has been carried out. The process involved three steps: synthesis of electroactive polymer microparticles with or without SiO_2, reduction of the electroactive polymer and uptake of palladium from acid solutions. The electroactive polymers used were polyaniline and polypyrrole, and the reduction of these polymers to their lowest oxidation state was essential for a substantial rate of uptake of palladium from the acid solution. The microparticles were characterized using X-ray photoelectron spectroscopy (XPS), BET surface area and particle size determination, thermogravimetric analysis and elemental analysis. The catalytic activities of the palladium-containing microparticles in the reduction of dissolved oxygen in water and the reduction of nitrobenzene to aniline were demonstrated.

Introduction

Electroactive polymers, such as polyaniline (PAN) and polypyrrole (PPY), have been shown to possess the ability to reduce and precipitate elemental gold from chloroauric acid solution.[1,2] The mechanism of gold reduction by PAN and PPY is postulated to be coupled with the changes in the oxidation states of these polymers and their protonation in acid solutions. Our initial work in this area was focused mainly on the use of electroactive polymer films. Recently we have also utilized microparticles of electroactive polymer–SiO_2 composites where the electroactive polymer components are present on the nano-scale (synthesized using the techniques of Armes *et al.*[3,4]) for the uptake of metal from acid solution.[5] These microparticles offer the distinct advantage of having a high surface area available for reaction. This would be particularly attractive for the synthesis of metal-containing composites for catalytic applications.

It has been postulated that electroactive polymers can be particularly attractive as host media for the confinement of catalyst particles since these media potentially provide an efficient route for the shuttling of electronic charges to the catalyst centers.[6] A vast majority of the prior work on electroactive polymer–metal catalyst composites involves the electrosynthesis of the polymer films and incorporation of catalyst particles which may be metal (*e.g.* platinum) or metal oxides (*e.g.* RuO_2). The catalytic particles may be electrodeposited onto a preformed polymer film[7–14] or incorporated into the polymer during synthesis.[6,15] The major disadvantage of using the former method is the possible confinement of the catalyst particles to the surface of the film or an uneven distribution of catalyst particles. In a recent work on the incorporation of platinum microparticles in an electrochemically grown PAN film, the use of dispersive X-ray spectroscopy has indicated that while a fairly constant Pt to C ratio is obtained across the 40 μm thick film, there is apparently some accumulation of platinum at the film/solution interface.[16] In our present work, we investigated the use of electroactive polymer microparticles as a host medium for palladium particles.

As mentioned earlier, the high surface area medium offered by the microparticles would be advantageous for the incorporation of catalytic particles and subsequent catalytic applications. Palladium catalysts can offer many advantages, *e.g.* no other transition metal is as versatile as palladium for C—C bond formations, palladium reagents show tolerance to many functional groups such as carbonyl and hydroxy groups, palladium is less expensive than Pt, Rh and Os and its toxicity has posed no problem so far.[17]

The emphasis of this paper is on the synthesis and characterization of the electroactive polymer–palladium microparticles. Various analytical techniques such as X-ray photoelectron spectroscopy (XPS), elemental analysis, particle size and surface area measurements were employed to characterize the microparticles. Preliminary results on the catalytic activity of these microparticles are also reported.

Experimental

Materials

Aniline (>99.5% purity) and pyrrole (>98% purity) were used as received (from Merck and BDH respectively) in the synthesis of polyaniline and polypyrrole, respectively. Colloidal silica (Ludox TMA, 34 wt.%, suspension in water, density 1.23 g cm^{-3}) and palladium chloride (5 wt.% solution in 10 wt.% HCl) were purchased from Aldrich Chemical Company. Ammonium persulfate [$(NH_4)_2S_2O_8$] and iron(III) chloride ($FeCl_3 \cdot 6H_2O$) were used as the oxidants for the polymerization of aniline and pyrrole, respectively.

Syntheses of PAN and PPY powders

Polyaniline (PAN) was synthesized in the following manner: 2 ml of aniline was pipetted into 100 ml of a 1 M HCl solution containing 3.14 g $(NH_4)_2S_2O_8$ with constant stirring. The reaction mixture was vigorously stirred for 16 h prior to filtration under reduced pressure. The collected solid particles were then washed with excess 1 M HCl and then dried under reduced pressure. In the synthesis of polypyrrole (PPY), 9.1 g of $FeCl_3 \cdot 6H_2O$ were added to 100 ml deionized water under constant stirring. After 1 h, 1 ml of pyrrole was pipetted into the aforementioned solution under vigorous stirring. After 16 h, the mixture was filtered and washed with excess deionized water and then dried under reduced pressure.

Preparation of PAN–SiO_2 and PPY-SiO_2 microparticles

PAN–SiO_2 microparticles were prepared as follows: 7.2 ml of colloidal silica was added to 100 ml of a 1.0 M HCl solution containing 3.14 g ammonium persulfate $(NH_4)_2S_2O_8$ at ambient temperature with constant stirring. Then, 2 ml of aniline was added and the solution turned green within four minutes.

---

†E-mail: chenkg@nus.edu.sg

This reaction mixture was vigorously stirred for 16 h. The colloidal suspension was then centrifuged at 9000 rpm for 15 min. The resulting dark green sediment was redispersed in 1 M HCl using an ultrasonic bath. This centrifugation–redispersion cycle was repeated twice more so as to remove the excess small silica particles from the PAN–SiO_2 microparticles. The microparticles were stored in suspension in 1 M HCl until subsequent use in the Pd uptake experiment. The PPY–SiO_2 microparticles were synthesized in the following manner: 7.2 ml of colloidal silica and 9.1 g of $FeCl_3 \cdot 6H_2O$ were added to 100 ml deionized water under stirring. After 1 h, 1 ml of pyrrole was pipetted into the above mentioned solution under vigorous stirring. The solution rapidly became dark. After 16 h, the solution was centrifuged at 9 000 rpm for 15 min. The resulting dark sediment was redispersed in deionised water using an ultrasonic bath. This centrifugation–redispersion cycle was repeated twice more as described for the PAN-SiO_2 microparticles, and the PPY–SiO_2 microparticles were stored in suspension in deionised water until subsequent use in the Pd uptake experiment.

The oxidation state of as-synthesized PAN in the form of powder or PAN–SiO_2 microparticles after undoping has been determined to be close to 50% (emeraldine). In the case of as-synthesized PPY, the corresponding oxidation state is 25%. Thus, the as-synthesized PAN–SiO_2 microparticles will be denoted as EM–SiO_2 in the subsequent discussion and PPY-SiO_2 will denote the as-synthesized microparticles with PPY existing in the 25% oxidized state. The fully reduced forms of PAN (leucoemeraldine or LM) and PPY (denoted as PPY°) were obtained by a two-step process. First, the EM and PPY powders and microparticles were undoped by treatment with excess 0.5 M NaOH for 1 h. In the second step, the powders and microparticles in the base form were reduced by treatment with hydrazine. The reduction was carried out at room temperature for 1 h using a weight ratio of hydrazine to microparticles of 2.5 to 1. The fully reduced powders and microparticles were then centrifuged and washed with deionised water and acetone until the excess hydrazine was removed.

Uptake of Pd from $PdCl_2$ solution

Palladium chloride in HCl (5 wt.% $PdCl_2$) was diluted to 100 mg dm^{-3} of palladium(II) ions in 0.5 M HCl. The PAN and PPY powders and microparticles were respectively added to 100 ml of the standard Pd solution under constant stirring. For both powders and microparticles, the initial molar ratios of N in PAN or PPY to Pd in solution were either 2:1 or 4:1. The Pd^{II} concentration in the solution was monitored as a function of reaction time using UV–VIS absorption spectroscopy (Shimadzu UV 160A scanning spectrophotometer). The absorbance at 280 nm was monitored and compared to the standard calibration curve of absorbance *versus* $PdCl_2$ concentration. After fixed periods of time, the powders and microparticles were removed from the $PdCl_2$ solution by centrifugation. The samples were washed with water and the centrifugation–washing cycle was carried out twice more. After drying, the samples were analyzed using a number of techniques (see below).

Catalytic activity of Pd-containing microparticles

The catalytic activity of the Pd-containing microparticles in the removal of dissolved oxygen in water was tested with 500 ml of deionised water at room temperature (23 °C) and 50 mg of the microparticles (Pd-free or with Pd) under constant stirring. H_2 or CO at 25 ml min^{-1} was continuously bubbled into the mixture. A YSI Model 50B Dissolved Oxygen Meter was used for measuring the oxygen concentration in the water at regular intervals. The catalytic activity of the Pd-containing microparticles in the hydrogenation of nitrobenzene to aniline was also investigated. The reaction was carried out at 30 °C with 1 mmol of nitrobenzene in ethanol and a Pd : nitrobenzene mole ratio of 1:100.

Characterization

Elemental analysis of the samples was carried on a Perkin-Elmer 2400CHN Elemental Analyzer with acetanilide as reference. Thermogravimetric analysis of the samples was carried out using a Netzsch STA409 to determine the polymer content in the microparticles. The samples were heated in air (100 ml min^{-1}) at a rate of 20 °C min^{-1} to 800 °C. The palladium content in the microparticles were determined using inductively coupled plasma emission spectrometry (ICP, Optima 3000DV from Perkin Elmer). Prior to this determination, the microparticles were subjected to a 1 h ultrasonic treatment with aqua regia to digest the Pd. The particle size distributions of the microparticles were measured using the Multi-Angle Sizing Option available with the Zeta Plus Analyzer from Brookhaven Instruments Corporation and their BET surface areas were determined using a Quantachrome Nova-1000. The adsorbate was N_2 and the 6-point BET method was used.

X-Ray photoelectron spectroscopy (XPS) was used to determine the surface composition of the samples. The measurements were made on a VG ESCALAB MKII spectrometer with a Mg-Kα X-ray source (1253.6 eV photons) at a constant retard ratio of 40. The samples were mounted on the standard sample studs by means of double-sided tape. The X-ray source was run at a reduced power of 120 W (12 kV and 10 mA). The pressure in the analysis chamber was maintained at 7.5×10^{-9} Torr or lower during each measurement. All binding energies (E_Bs) were referenced to the C 1s neutral carbon peak at 284.6 eV. In peak synthesis, the linewidth (full width at half maximum, FWHM) for the Gaussian peaks was maintained constant for all components in a particular spectrum. Surface elemental stoichiometries were determined from peak-area ratios, after correcting with the experimentally determined sensitivity factors, and were reliable to $\pm 10\%$. The elemental sensitivity factors were determined using stable binary compounds of well established stoichiometries.

The reaction products after the catalytic hydrogenation of nitrobenzene were identified by gas chromatography using a Perkin Elmer Auto System XL equipped with a 30 m poly(methylsiloxane) fused silica column (from Supelco) and a flame ionization detector.

Results and Discussion

Properties of electroactive polymer–SiO_2 microparticles

The polymer content of the microparticles as determined by thermogravimetric analysis, and the chemical composition as determined by XPS and elemental analyses are given in Table 1. The C/N ratios of the EM–SiO_2 and LM–SiO_2 particles determined from XPS and elemental analysis are close to that expected of PAN (6.0) and those of PPY–SiO_2 and PPY°–SiO_2 are close to that expected of PPY (4.0). The Cl/N ratios of the EM–SiO_2 and PPY–SiO_2 microparticles are similar to those reported earlier for EM and PPY with Cl^- counterions.[18,19] The Cl/N ratios of the LM–SiO_2 and PPY°–SiO_2 are much lower since these samples have been undoped. The surface Si/N ratios as determined by XPS are very much higher compared to the bulk composition values estimated from thermogravimetric analysis (bulk Si/N ≈1.3–1.9), confirming a SiO_2-rich surface. From Table 1 it can be seen that there is some loss of SiO_2 or SiO_2-rich material during the process of reducing the polymer to the lowest oxidation state. This loss is greater when EM–SiO_2 is converted to LM–SiO_2 than when the PPY–SiO_2 is converted to PPY°–SiO_2, and the loss of SiO_2 in the former case is predominantly from the surface.

Table 1 Chemical composition, effective particle size and specific surface area of electroactive polymer–SiO_2 microparticles

		XPS analysis			bulk analysis				
type of microparticles	polymer content (wt.%)	C/N	Cl/N	Si/N	C/N	H/N	Si/N	particle size/nm	specific surface area/m^2 g^{-1}
EM–SiO_2	42.4	6.1	0.35	10.8	6.1	4.5	1.93	530	72.1
LM–SiO_2	52.7	6.1	0.03	4.70	6.0	5.2	1.32	490	61.2
PPY–SiO_2	37.8	4.7	0.23	11.1	3.8	3.6	1.83	320	91.2
PPY°–SiO_2	42.5	4.2	0.08	10.0	4.0	4.2	1.51	320	90.4

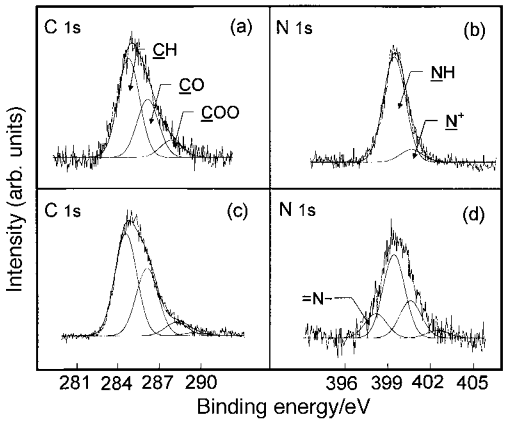

Fig. 1 XPS C 1s and N 1s core level spectra of [(a) and (b)] LM–SiO_2 and [(c) and (d)] Pd–LM–SiO_2 obtained after reaction in $PdCl_2$ solution (100 mg dm^{-3} Pd^{2+} in 0.5 M HCl, 40 h, initial N/Pd = 4 : 1)

The curve-fitted C 1s and N 1s core-level spectra of the LM–SiO_2 microparticles and the PPY°-SiO_2 microparticles are shown in Fig. 1 and 2 respectively. The corresponding spectra for EM–SiO_2 and PPY–SiO_2 have been reported earlier.[5] The C 1s core-level spectra [Fig. 1(a) and 2(a)] show the presence of oxidized carbon species, predominantly C—O groups [at a binding energy (E_B) of 286.0 eV][20] and the proportion of oxidized C species is higher for PPY° than LM. The N 1s core-level spectrum of the LM–SiO_2 [Fig. 1(b)] shows a major component at 399.4 eV attributed to -NH- and a small peak component around 401 eV attributed to N^+. This is consistent with the structure of LM.[21] In the case of PPY°, the great propensity for the fully reduced PPY to react with oxygen[22] results in a significant amount of positively charged species (N^+) [Fig. 2(b)]. The intensities of the C 1s and N 1s spectra of PPY°–SiO_2 are much weaker than those of LM–SiO_2 (Fig. 2) due to the higher concentration of SiO_2 in the surface region of the former (Table 1).

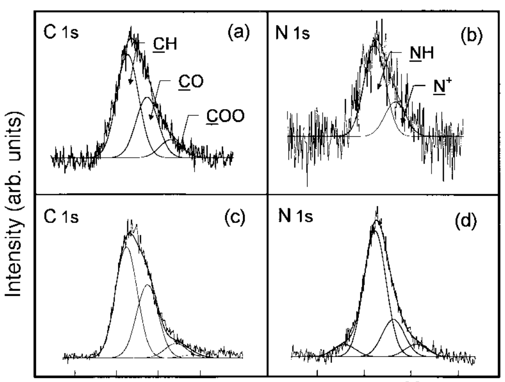

Fig. 2 XPS C 1s and N 1s core level spectra of [(a) and (b)] PPY°–SiO_2 and [(c) and (d)] Pd–PPY°–SiO_2 obtained after reaction in $PdCl_2$ solution (100 mg dm^{-3} Pd^{2+} in 0.5 M HCl, 40 h, initial N/Pd = 4 : 1)

The effective particle sizes determined in this work (based on the light scattering technique) are about twice those reported by Maeda and Armes for EM–SiO_2 and PPY–SiO_2 microparticles having similar polymer contents[23] (Table 1). The differences in the type of colloidal silica and techniques employed in the determinations of particle size may result in the differences in value, especially since the light scattering technique is sensitive to the presence of aggregates. The colloidal silica used in this work has an effective diameter of 180 nm which is significantly larger than those used by Armes *et al.* (reported to be 38 nm).[4] A slight decrease in particle size of the LM–SiO_2 microparticles compared to EM–SiO_2 microparticles is observed (Table 1), consistent with the loss of material. The LM and PPY° powders synthesized in the absence of SiO_2 have mean particle sizes about 2 to 3 times those of the corresponding microparticles with SiO_2. The specific surface areas of the microparticles as determined by the BET technique (Table 1) are about an order of magnitude higher than those based on the particle size and assuming a spherical morphology and a particle density of 2 g cm^{-3},[23] indicating a high degree of porosity in the microparticles.

Uptake of Pd from solution

Fig. 3 shows the decrease in the concentration of $PdCl_2$ in acid solution (as measured by the decrease in the absorption of the 280 nm band) as a function of reaction time with PAN in the EM and LM oxidation state in either the powder form or as SiO_2-containing microparticles. It can be clearly seen that PAN in the fully reduced LM state is much more effective than the EM state (50% oxidation) in the uptake of Pd from the solution. The use of LM–SiO_2 microparticles resulted in a higher rate and extent of Pd uptake than LM powder (of the same weight as the LM in the microparticles). From the experiment conducted with SiO_2 alone (Fig. 3), it can be conclude that the SiO_2 plays no direct role in the reaction with Pd. The higher efficiency observed with the LM–SiO_2 microparticles as compared to LM powder is thus attributed to the larger surface available for reaction in the former

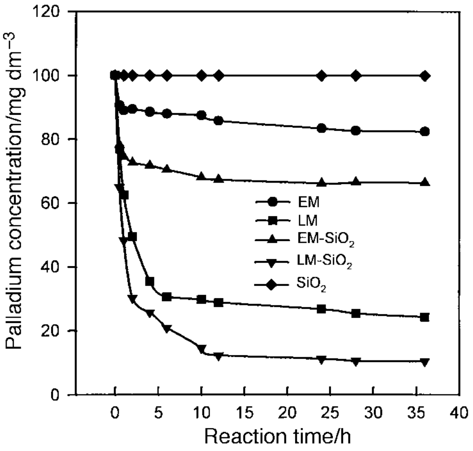

Fig. 3 Effect of PAN in various oxidation states and forms on $PdCl_2$ concentration in acid solution. Initial N/Pd = 4 : 1.

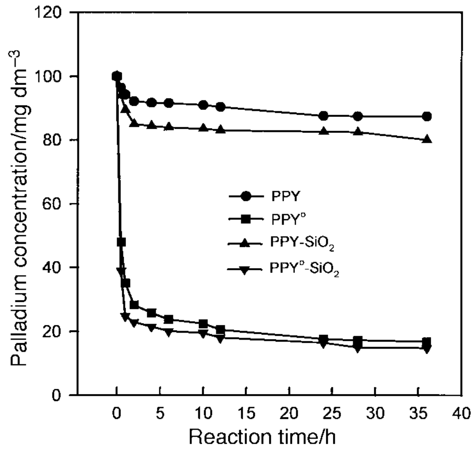

Fig. 4 Effect of PPY in various oxidation states and forms on $PdCl_2$ concentration in acid solution. Initial N/Pd = 4 : 1.

(specific area of LM–SiO_2 is 61.2 m^2 g^{-1} compared to 49.5 m^2 g^{-1} for LM) even though the XPS results show a SiO_2-rich surface. Similarly, the EM–SiO_2 microparticles are more effective in Pd uptake than EM powder.

Fig. 4 shows the rate of Pd uptake by PPY in the various oxidation states and forms. Similar to the results obtained with PAN, the fully reduced PPY° in either powder or microparticle form is more effective than the 25% oxidized form. The rate and extent of reaction obtained with the microparticles are also higher than those obtained with the powders. This is again attributed to the larger surface area in the microparticles (90.4 m^2 g^{-1} for PPY°–SiO_2 compared to 9.3 m^2 g^{-1} for PPY° powder).

In the case of LM–SiO_2 and PPY°–SiO_2, the effect of the N/Pd ratio of the reactants on the rate of Pd uptake is shown in Fig. 5. The initial rate is rapid when a reactant N/Pd ratio of either 2 or 4 is used but the rates after the first hour slow down substantially. The asymptotic amount of Pd uptake with an initial reactant N/Pd ratio of 4 is less than twice that observed when the N/Pd ratio is halved. It is suspected that a substantial amount of LM and PPY° in the bulk of the microparticles may not be readily accessible for reaction with the $PdCl_2$.

The C 1s and N 1s core-level spectra of LM–SiO_2 microparticles after 40 h in the $PdCl_2$ solution (100 mg dm^{-3} Pd^{2+} in 0.5 M HCl, initial N/Pd = 4 : 1) are shown in Fig. 1(c) and (d) respectively while the corresponding spectra for PPY°–SiO_2 are shown in Fig. 2(c) and (d) respectively. The results show that the proportions of oxidized C species in both the LM–SiO_2 and PPY°–SiO_2 microparticles increase after reaction in the $PdCl_2$ solution. In Fig. 1(d) and 2(d), a peak component is present at the low E_B side of the -NH- peak. This peak is attributed to the -N=groups.[17] The microparticles after reaction in the $PdCl_2$ solution were centrifuged and washed with copious amounts of water. The unprotonated -N=groups result from a certain amount of undoping which occurred during the washing process. The -N=/N ratio of the LM–SiO_2 microparticles after reaction in $PdCl_2$ has increased to 0.19, indicating an increase in oxidation state. A similar observation can be made with the PPY°–SiO_2 microparticles. The compositions of the LM–SiO_2 and PPY°–SiO_2 microparticles after reaction in $PdCl_2$ solution (N/Pd = 4 : 1, 40 h) are shown in Table 2. While the C/N ratios of the LM–SiO_2 and PPY°–SiO_2 microparticles obtained from elemental analysis are again close to the value of the pristine samples, the thermogravimetric analysis shows that the organic fraction has increased, contrary to what is expected if there is uptake of Pd by the microparticles. It is postulated that during the uptake reaction, the microparticles lose a part of the SiO_2-rich fraction (surface region) which remained too fine to be efficiently collected after the centrifugation and washing process. This loss of the SiO_2-rich fraction together with the accumulated Pd results in the Pd/N ratio in the collected microparticles (Table 2) being lower than what would be expected from the decrease in the $PdCl_2$ concentration in solution (Fig. 3 and 4). The microparticles that were collected are about three times larger than the particles before Pd uptake and the specific surface area has also decreased by approximately a factor of 3 (Table 2). It is possible that with the loss of the SiO_2-rich surface layer, the particles are prone to agglomeration and hence the increase in particle size.

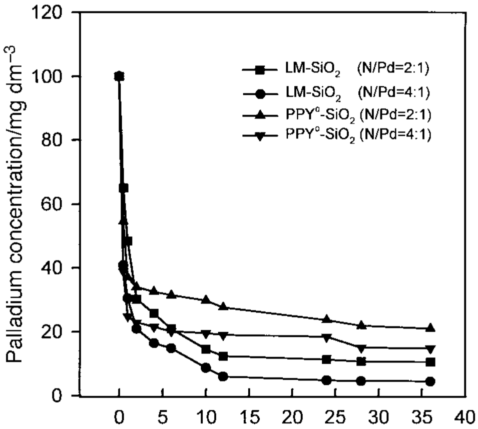

Fig. 5 Effect of loading of LM–SiO_2 and PPY°–SiO_2 on $PdCl_2$ concentration in acid solution

The Pd 3d core-level spectra of the LM–SiO_2 and PPY°–SiO_2 microparticles after reaction in the acidic $PdCl_2$ solution show a Pd $3d_{5/2}$ peak component around 337.5 eV [Fig. 6(a) and (c) respectively], characteristic of Pd^{II}.[24] Thus, the Pd from solution was not reduced to Pd^0 (which would have a Pd $3d_{5/2}$ peak component around 335 eV[24]), unlike the case of Au uptake from acidic $AuCl_3$ solution.[1,2] The Cl 2p core-level spectra of the LM–SiO_2 and PPY°–SiO_2 microparticles after Pd uptake [Fig. 6(b) and (d) respectively] show a predominant peak component around 198 eV. The position of this peak agrees with the corresponding Cl 2p peak component of $PdCl_2$ used for calibration. From Table 2, it can be seen that the Cl/Pd ratios in both types of microparticles are around 2, which strongly indicates that the Pd is present as $PdCl_2$ in the microparticles. The Pd content in the microparticles is not significantly affected by soaking the microparticles in water for 24 h. The mechanism of Pd uptake is not clear at present but it is probable that $PdCl_2$ from the solution forms a complex with LM and PPY° (but not so readily with the higher oxidation states of PAN or PPY). The ability of palladium chloride and platinum chloride (in the form of Pd_6Cl_{12} and Pt_6Cl_{12}, respectively) to bind with electron donors has been reported.[25]

The XPS results of LM and PPY° powder (without SiO_2) after the $PdCl_2$ uptake experiments confirmed the existence of Pd predominantly as Pd^{2+}. A Cl/Pd ratio of close to 2 is also obtained. With the assumption that the Pd exists as $PdCl_2$ in the LM and PPY° powders after the uptake experiments, a comparison was made of the amount of $PdCl_2$ taken up from solution (as measured by UV–VIS absorption spectroscopy) and the equivalent amount on the powders (estimated by both TG and ICP measurements). In contrast to the results obtained with the SiO_2-containing microparticles, all three techniques gave consistent results (within 8% of the average value) for the LM and PPY° powders.

Catalytic activity of Pd-containing microparticles

The catalytic activity of Pd-containing LM–SiO_2 microparticles in the removal of dissolved oxygen in water by reduction

Table 2 Chemical composition, effective particle size and specific surface area of electroactive polymer–SiO_2 microparticles after Pd uptake

type of microparticles	organic fraction			Pd content			particle size/nm	specific surface area/ $m^2\ g^{-1}$
	wt.%[a]	Cl/N (bulk)	H/N (bulk)	Pd/N (XPS)	Cl/Pd (XPS)	wt.%[b]		
LM–SiO_2	89.2	6.1	4.0	0.10	2.6	4.3	1500	20.4
PPY°–SiO_2	86.6	4.0	2.7	0.08	1.9	4.7	960	32.5

[a] From thermogravimetric analysis. [b] From inductively coupled plasma analysis.

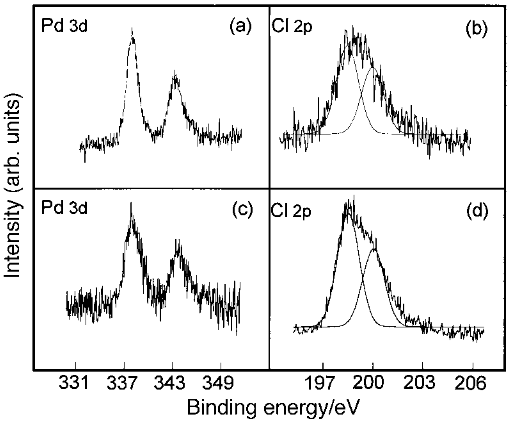

Fig. 6 XPS Pd 3d and Cl 2p core-level spectra of [(a) and (b)] Pd–LM–SiO_2 and [(c) and (d)] Pd–PPY°–SiO_2, obtained after reaction in $PdCl_2$ solution (100 mg dm^{-3} Pd^{2+} in 0.5 M HCl, 40 h, initial N/Pd = 4 : 1)

with H_2 is demonstrated by the results in Fig. 7. By comparing the results obtained with and without the LM–SiO_2 microparticles, it can be concluded that even in the absence of Pd, reduction in dissolved oxygen content can be achieved with LM–SiO_2. In the presence of Pd, the reduction of dissolved oxygen is greatly accelerated and a reduction of the dissolved oxygen concentration from an initial value of 8.6 ppm to less than 100 ppb is easily achieved with 0.01 wt.% of the Pd containing microparticles in the water. With PPY°–SiO_2 microparticles, the efficiency in reducing the dissolved oxygen content is slightly lower.

The catalytic activity of the Pd-containing microparticles was also tested in the hydrogenation of nitrobenzene to aniline. Fig. 8(a) shows the chromatogram of a calibration mixture of 1 mmol each of aniline and nitrobenzene in 20 ml of ethanol, while Fig. 8(b) shows the chromatogram of the products of the reaction mixture containing 1 mmol of nitrobenzene and the LM–SiO_2 microparticles containing 4.3 wt.% Pd (Pd/nitrobenzene = 1/100 mole basis) in 20 ml of ethanol after hydrogenation for 2 h at 30 °C. As shown in Fig. 8(b) there is almost a complete conversion of the nitrobenzene to aniline. The catalytic activity of the LM in the hydrogenation of nitrobenzene was shown to be negligible.

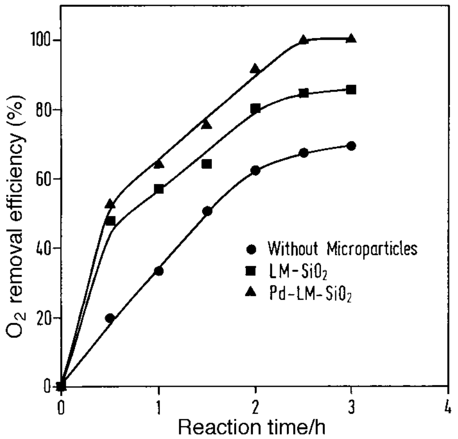

Fig. 7 Effect of LM–SiO_2 with and without Pd on the reduction of dissolved oxygen concentration in water by H_2 (0.01 wt% microparticles in H_2O used)

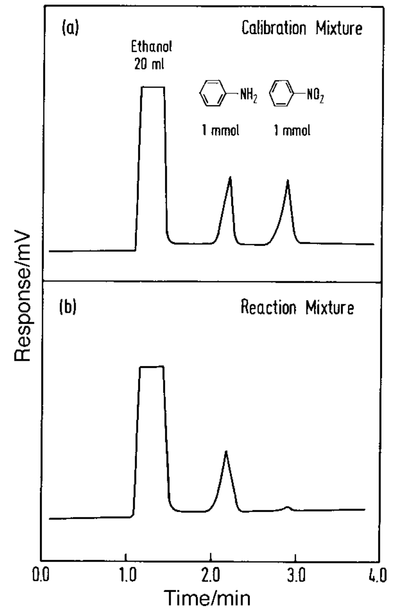

Fig. 8 Chromatograms showing (a) a calibration mixture of 1 mmol of nitrobenzene and 1 mmol of aniline in 20 ml ethanol and (b) composition of reaction mixture containing 1 mmol of nitrobenzene and Pd–LM–SiO_2 (Pd/nitrobenzene = 1/100 mole basis) in 20 ml ethanol after hydrogenation for 2 h

Conclusion

Polyaniline and polypyrrole are capable of reacting with $PdCl_2$ in acidic solution resulting in the uptake of Pd from the solution. The reactions are rapid when these electroactive polymers are reduced to their lowest oxidation states. The electroactive polymers synthesized in the form of SiO_2-containing nanocomposites offer a larger specific surface area and a higher reaction rate for uptake reactions with $PdCl_2$ as compared to the electroactive polymer in powder form without SiO_2. However, in the course of the reactions, the SiO_2-containing microparticles exhibit some loss of their SiO_2-rich surface region. XPS analysis shows that the Pd accumulated by the microparticles exists as Pd^{2+} and most probably as $PdCl_2$, rather than elemental Pd. The catalytic activities of the Pd-containing electroactive polymer microparticles are demonstrated by the removal of dissolved oxygen from water and in the hydrogenation of nitrobenzene to aniline.

References

1 E. T. Kang, Y. P. Ting, K. G. Neoh and K. L. Tan, *Synth. Met.*, 1995, **69**, 477.
2 Y. P. Ting, K. G. Neoh, E. T. Kang and K. L. Tan, *J. Chem. Technol. Biotechnol.*, 1994, **39**, 31.
3 S. Maeda and S. P. Armes, *J. Colloid Interface Sci.*, 1993, **159**, 257.

4 M. Gill, J. Mykytiuk, S. P. Armes, J. L. Eduards, T. Yeates, P. J. Moreland and C. Mollet, *J. Chem. Soc., Chem. Commun.*, 1992, 108.

5 K. G. Neoh, K. K. Tan, P. L. Goh, S. W. Huang, E. T. Kang and K. L. Tan, *Polymer*, submitted.

6 K. Rajeshwar and C. S. C. Bose, *US Patent*, 5 334 292, 1994.

7 G. K. Chandler and D. Pletcher, *J. Appl. Electrochem.*, 1986, **16**, 62.

8 A. Leone, W. Marino and B. R. Scharifker, *J. Electrochem. Soc.*, 1992, **139**, 438.

9 D.E. Bartak, B. Kazee, K. Schimazu and T. Kuwana, *Anal. Chem.*, 1986, **58**, 2756.

10 G. Tourillon, E. Dartyge, H. Dexpert, A. Fontaine, P. Jucha, P. Lagarde and D. E. Sayers, *J. Electroanal. Chem.*, 1984, **178**, 357.

11 M. Gholamian and A. Q. Contractor, *J. Electroanal. Chem.*, 1990, **289**, 69.

12 K. M. Kost, D. E. Bartak, B. Kazee and T. Kuwana, *Anal. Chem.*, 1988, **60**, 239.

13 S. Holdowft and B. L. Funt, *J. Electroanal. Chem.*, 1988, **240**, 89.

14 F. T. A. Vork, L. J. J. Janssen and E. Barendrecht, *Electrochim. Acta*, 1986, **31**, 1569.

15 R. Noufi, *J. Electrochem., Soc.*, 1983, **130**, 2126.

16 R. Kostecki, M. Ulmann, J. Augustynski, D. J. Strike and M. Koudelka-Hep, *J. Phys. Chem.*, 1993, **97**, 8113.

17 J. Tsuji, *Palladium Reagents and Catalysts: Innovations in Organic Synthesis*, John Wiley, Chichester, 1995, p. 1.

18 K.L. Tan, B. T. G. Tan, E. T. Kang and K. G. Neoh, *Phys. Rev. B*, 1989, **39**, 8070.

19 E. T. Kang, K. G. Neoh and K. L. Tan, in *Handbook of Organic Conductive Molecules and Polymers*, ed. H. S. Nalwa, John Wiley & Sons, Chichester, 1997, vol. 3, ch. 3, pp. 121–181.

20 *Handbook of X-ray Photoelectron Spectroscopy*, ed. J. Chastain, Perkin-Elmer, Eden Prairie, MN, 1992, p. 41.

21 K. G. Neoh, E. T. Kang and K. L. Tan, *J. Polym. Sci. A: Polym. Chem.*, 1991, **29**, 759.

22 G. B. Street, T. C. Clarke, M. Krounbi, K. Kanazawa, V. Lee, P. Pfluger, J. C. Scott and G. Weiser, *Mol. Cryst. Liq. Cryst.*, 1982, **83**, 253.

23 S. Maeda and S. P. Armes, *Synth. Met.*, 1995, **73**, 151.

24 *Handbook of X-ray Photoelectron Spectroscopy*, ed. J. Chastain, Perkin-Elmer, Eden Prairie, MN, 1992, p. 119.

25 P. M. Maitlis, *The Organic Chemistry of Palladium, vol. I: Metal Complexes*, Academic Press, New York, 1971, p. 45.

Paper 8/02245C; *Received* 23rd March, 1998